Kinetics of the formation process of PbO_2 on lead–antimony electrodes

Guo-Lin Wei*, Jia-Rong Wang

Department of Chemistry, Shanghai University of Science and Technology, Jiading, Shanghai 201800, China

Abstract

The kinetics of the formation process of PbO_2 on Pb–1wt.%Sb and Pb–7wt.%Sb electrodes, together with the influence of antimony on this process, are studied with potential-step and a.c. impedance methods. Relationships between the current density and time, and between the capacitance and time, are investigated. The oxidation current of the lead substrate is considered. Results show that the formation process of PbO_2 on lead–antimony electrodes follows a two-dimensional instantaneous nucleation/growth process. Antimony enhances the formation of PbO_2 nuclei, but inhibits their growth.

Keywords: Electrodes; Lead; Antimony; Formation process

1. Introduction

Because of the importance to the performance of lead/acid batteries, both the oxidation process of $PbSO_4$ to PbO_2 on a lead electrode [1,2] and the influence of antimony on the characteristics of the positive plate [3,4] have been widely studied. The growth process of PbO_2 on lead–antimony electrodes, however, has still to be examined in detail [5]. Valeriote and Gallop [1] concluded that the oxidation process of $PbSO_4$ to PbO_2 on a pure-lead electrode involves sequentially three diffusion processes, followed by, at least two electro-crystallization stages and a further diffusion process. By contrast, Dawson et al. [2] considered the mechanism to be a three-dimensional continuous nucleation and growth process that operates under diffusion control. For cycled lead–antimony electrodes, Hameenoja and Hampson [5] claimed the oxidation process to have an intermediate two- and three-dimensional character. The influence of the oxidation current of the lead substrate has not been taken into account in the above papers and this probably causes the differences in the conclusions. As for the effect of antimony on the formation of PbO_2, it was suggested by Ritchie and Burbank [3] that antimony acts as a nucleating catalyst for PbO_2 and, at the same time, inhibits the crystal growth. It

should be pointed out, however, that no evidence was presented in support of these conclusions. In the present work, the kinetics of the formation process of PbO_2 on lead–antimony electrodes and the effect of antimony on this process have been investigated further.

2. Experimental

A.c. impedance tracing measurements were performed with a frequency response analyser (Solartron 1250) and an electrochemical interface (Solartron 1186). A 10 mV (peak-to-peak) sine-wave perturbing signal with a frequency of 1000 Hz was used. The impedance is represented by an equivalent circuit that is composed of a resistance, Rs, and a capacity, Cs, in series. Other instruments used included a JH-2C potentiostatic, an XFD-8A super-low frequency signal generator and an LZ3-204 recorder. All experiments were carried out at 30 ± 0.1 °C.

The electrodes under investigation were Pb–1wt.%Sb and Pb–7wt.%Sb rods that were sealed with epoxy resin at the lower part of an L-shaped glass tube to give an exposed area of 0.28 cm^2. The counter electrode was a Pt plate with dimensions of 1 cm × 1 cm. The reference electrode was an Hg/Hg_2SO_4 electrode that contained the same solution as that in the cell. The H_2SO_4 solution was prepared from AR grade H_2SO_4 and double-distilled water.

*Corresponding author.

The working electrode was polished carefully with emery papers before each experiment. It was maintained in 4.5 M H_2SO_4 at 1.3 V (versus Hg/Hg_2SO_4) for 20 min and then at 0.9 V for 5 min. The electrode potential was then stepped to 1.4 or 1.3 V and the i–t transient or impedance curve result was recorded.

Linear sweep voltammetry at a scan rate of 9.5 mV s^{-1} was used as an in situ quantitative analysis method to determine the phase composition of the lead anodic film that formed during pretreatment of the test electrode [6]. Table 1 shows the results for an electrode after being polarized at 1.3 V for 20 min. Q_a, Q_b, Q_c and Q_d correspond, respectively, to the charge densities required to reduce PbO_2 (to $PbSO_4$, $E_p = 1.05$ V), PbO and $PbO \cdot PbSO_4$ (both to Pb, $E_p = -0.90$ V), $PbSO_4$ (to Pb, $E_p = -1.02$ V) and Sb_2O_3 (to Sb, $E_p = -0.60$ V). After being polarized at 0.9 V for 5 min, the PbO_2 composite is reduced to $PbSO_4$.

3. Results and discussion

3.1. Potential-step method

Fig. 1 shows the typical current–time transient after the electrode potential was stepped from 0.9 to 1.4 or 1.3 V. There is an obvious current peak (M) on the curve. This can be ascribed to a PbO_2 nucleation and growth process. Before this process, the current arises mainly from the oxidation of the lead substrate. The current density, i_1, is proportional to $t^{-1/2}$ [7]:

$$i_1 = a_1 + a_2 t^{-1/2} \tag{1}$$

where a_1 and a_2 are constants.

Table 2 shows the linear results for this time range, E is the potential to which the electrode is stepped from 0.9 V, T is the time range for calculation, and R is the correlation coefficient.

For the formation process of PbO_2, considering the two-dimensional instantaneous nucleation and growth process with the overlapping of nuclei, the current density can be represented as [8,9]:

$$i_2 = 2nF\pi(M/\rho)hk^2N_0t \ \exp(-\pi M^2k^2N_0t^2/\rho^2) \tag{2}$$

where n is the number of electrons transferred, F is the Faraday constant, M and ρ are the molar mass and density of PbO_2, respectively; h and k are the height
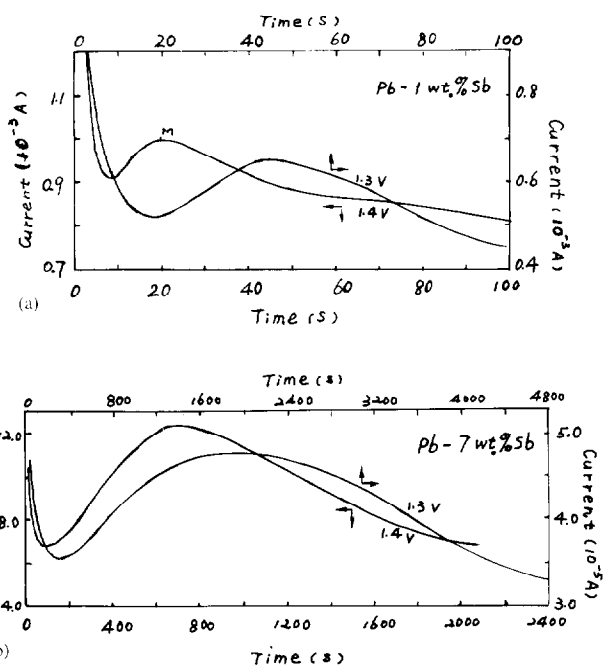

Fig. 1. Current–time transients after electrode potential stepped from 0.9 V to that shown on the curves: (a) Pb–1wt.%Sb, and (b) Pb–7wt.%Sb.

Table 2
Results for i_1 vs. $t^{-1/2}$

Electrode	E (V)	T (s)	a_1 (A cm^{-2})	a_2 (A cm^{-2} s$^{-1/2}$)	R
Pb–1wt.%Sb	1.4	2.0–5.0	9.71×10^{-4}	5.49×10^{-3}	1.0000
	1.3	3.0–8.0	3.08×10^{-4}	5.29×10^{-3}	0.9982
Pb–7wt.%Sb	1.4	22.0–58.0	1.37×10^{-4}	8.02×10^{-4}	0.9992
	1.3	20.0–144	0.999×10^{-4}	4.34×10^{-4}	0.9998

and the growth rate constant of the two-dimensional nucleus, respectively, N_0 is the initial number of nuclei. Eq. (2) can be written as:

$$\ln(i_2/t) = b_1 - b_2t^2 \tag{3}$$

with

$$b_1 = \ln[2nF\pi(M/\rho)hk^2N_0] \tag{4}$$

$$b_2 = \pi M^2k^2N_0/\rho^2 \tag{5}$$

The maximum current value of i_2, according to Eq. (2), corresponds to:

$$t_m = 1/(2b_2)^{1/2} \tag{6}$$

$$(i_2)_m = \exp(b_1)/(2eb_2)^{1/2} \tag{7}$$

The apparent current density near the current peak M in Fig. 1 can be represented as the summation of two parts:

$$i = i_1 + i_2 \tag{8}$$

Table 1
Reduction charge densities of a lead anodic film formed by polarizing electrode at 1.3 V for 10 min; scan range: +1.3 to −1.3 V; scan rate: 9.5 mV s^{-1}

Electrode	Q_a (mC cm^{-2})	Q_b (mC cm^{-2})	Q_c (mC cm^{-2})	Q_d (mC cm^{-2})
Pb–1wt.%Sb	44.5	124	149	
Pb–7wt.%Sb	3.62	83.4	116	13.0

Eq. (3) can then be written as:

$$\ln[(i-i_1)/t] = b_1 - b_2 t^2 \tag{3'}$$

Thus, there should be a good linearity between $\ln[(i-i_1)/t]$ and t^2 on either side of the formation current peak M. This is demonstrated in Table 3. At shorter (before $t_m/2$) or longer (after $2t_m$) time, i_2 is so small that the error caused by i_1 cannot be corrected adequately. The oxygen-evolution current will be appreciable after $2t_m$ in comparison with i_2. As a consequence, the linearity will not be maintained in these time ranges.

Other electrocrystallization processes (such as two-dimensional progressive nucleation and growth process, three-dimensional instantaneous or progressive nucleation and growth process with or without control by the diffusion process) have been also used to model the curves in Fig. 1. The theoretical results, however, are in poor agreement with the experimental results. It may be concluded, therefore, that with the consideration of the oxidation current of the lead substrate, the formation process of PbO_2 on lead–antimony electrodes is a two-dimensional instantaneous nucleation and growth process.

It can be seen from Eqs. (4) and (5) that the height of the nucleus, h, increases with $\exp(b_1/b_2)$ and the growth rate constant, k, increases with b_2. Values for $\exp(b_1/b_2)$ and b_2 are listed in Table 3. For the same potential, $\exp(b_1/b_2)$ increases with the amount of antimony, but b_2 decreases. Thus, h is larger for a Pb–7wt.%Sb electrode than that for a Pb–1wt.%Sb electrode, but k is smaller. This means that antimony in the positive grid alloy will enhance the formation of the PbO_2 nucleus, but will inhibit its growth. A dense and tenacious PbO_2 film that cannot be reduced to $PbSO_4$ easily may be formed on a Pb–7wt.%Sb electrode. This may provide an explanation for the premature capacity loss phenomenon that occurs when the antimony content in the positive grid alloy of a lead/acid battery is <1.5 wt.% [10].

3.2. Impedance method

The C_s obtained in the present work has an order of magnitude of mF cm^{-2}. This is much larger than that of an ordinary double layer that has an order of

magnitude of μF cm^{-2}. Thus, C_s is due to the PbO_2 composite and will increase with its quantity. Table 4 lists the C_s values obtained at different stages, where C_{s0}, C_{s1} and C_{s2} represent, respectively, the C_s value obtained after polarizing the electrode at 1.3 V for 20 min, after polarizing the electrode at 0.9 V for 5 min, and after the potential is stepped to a value E for a time t.

After polarizing the electrode at 0.9 V for 5 min, PbO_2 formed in the lead anodic film at 1.3 V will be reduced. Thus, the value of C_{s1} is much smaller than that of C_{s0}. Nevertheless, it is still much larger than that of an ordinary double layer. There may exist some unreduced PbO_2 that may act as nuclei during the succeeding nucleation and growth process of PbO_2 after the potential step to 1.4 or 1.3 V.

From Eqs. (3) and (6), it is possible to derive the charge consumed in the formation of PbO_2, i.e.:

$$Q = \int_0^t i_2 \, dt = \exp(b_1/2b_2)[1 - \exp(-t^2/2t_m^2)] \tag{9}$$

Since C_{s2} is proportional to the surface area of PbO_2, it can be assumed that:

$$C_{s2} = C_s^0 + K[1 - \exp(-t^2/2t_m^2)]^{2/3} \tag{10}$$

where C_s^0 and K are constants. Thus:

$$dC_{s2}^2/dt^2 = 2K/3t_m^2[1 - \exp(-t^2/2t_m^2)]^{-1/3} \exp(-t^2/2t_m^2)$$
$$\times \{1 - t^2/t_m^2 - 1/3[1 - \exp(-t^2/2t_m^2)]^{-1}$$
$$\times \exp(-t^2/2t_m^2)(t^2/2t_m^2)\} \tag{11}$$

Assuming that $dC_{s2}^2/dt^2 = 0$, Eq. (11) becomes:

$$[1 - \exp(-t^2/2t_m^2)]^{-1/3} \exp(-t^2/2t_m^2)$$
$$\times \{1 - t^2/t_m^2 - 1/3[1 - \exp(-t^2/2t_m^2)]^{-1}$$
$$\times \exp(-t^2/2t_m^2)(t^2/2t_m^2)\} = 0 \tag{12}$$

A reasonable approximate solution of this equation is $t \approx 0.63t_m$. The left side of this equation is larger than 0 when $t < 0.63t_m$ and is smaller than 0 when $t > 0.63t_m$. Thus, the increasing rate of C_{s2} reaches the maximum value at $0.63t_m$. By using Eq. (6), the b_2 value can be obtained from the time value that corresponds to this maximum increasing rate of C_{s2}. The values are given

Table 3
Results for $\ln[(i-i_1)/t]$ vs. t^2

Electrode	E (V)	T (s)	b_1 (ln(A cm^{-2} s^{-1}))	b_2 (s^{-2})	R	$\exp(b_1/b_2)$ (C cm^{-2})
Pb–1wt.%Sb	1.4	13.2–44.0	−9.43	4.93×10^{-4}	0.9983	0.163
	1.3	27.0–86.5	−10.2	1.87×10^{-4}	0.9992	0.198
Pb–7wt.%Sb	1.4	290–1420	−14.4	8.60×10^{-7}	0.9983	0.648
	1.3	970–4000	−16.8	1.29×10^{-7}	0.9990	0.392

Table 4
C_s values at different electrode potentials

Electrode	Pb–1wt.%Sb				Pb–7wt.%Sb			
E (V)	1.4		1.3		1.4		1.3	
C_{s0} (mF cm^{-2})	5.31		5.44		0.220		0.212	
C_{s1} (mF cm^{-2})	0.162		0.159		0.0668		0.0619	
	t (s)	C_{s2} (mF cm^{-2})	t (s)	C_{s2} (mF cm^{-2})	t (s)	C_{s2} (mF cm^{-2})	t (s)	C_{s2} (mF cm^{-2})
	10	2.39	10	1.68	15	0.300	30	0.327
	20	3.27	20	2.04	150	0.655	300	0.689
	30	3.97	30	2.73	300	1.35	600	1.12
	40	4.56	40	3.38	390	1.94	750	1.38
	60	5.23	60	4.16	480	2.33	870	1.74
	100	6.05	100	5.54	600	2.80	1050	2.16
					750	3.30	1350	2.76
					900	3.67	1500	3.01

Table 5
Values of b_2 obtained with impedance method and the calculated results for C_{s2} and t

Electrode	Pb–1wt.%Sb		Pb–7wt.%Sb	
E (V)	1.4	1.3	1.4	1.3
$0.63t_m$ (s)	20	30	390	870
b_2 (s^{-2})	4.96×10^{-4}	2.21×10^{-4}	1.31×10^{-6}	2.62×10^{-7}
C_s^0 (mF cm^{-2})	1.90	1.26	0.320	0.255
K (mF cm^{-2})	4.03	4.55	4.63	4.72
R	0.9968	0.9977	0.9965	0.9989

in Table 5 and are very close to that obtained from the potential-step method (Table 3). The difference is probably caused by the pretreatment process of the electrode.

The relationship between C_{s2} and t can be modelled with b_2 values obtained from the impedance method, as given by Eq. (10). It can be seen from Table 5 that the data fit well Eq. (10). C_s^0 represents C_{s2} immediately after the potential has stepped. In general, C_{s2} is a little smaller than the first value of C_{s2} shown in Table 4. K represents the increasing rate of C_{s2} with the t/t_m value and/or with the amount of PbO$_2$ formed. It is larger for a Pb–7wt.%Sb electrode than for Pb–1wt.%Sb electrode. This is probably because the PbO$_2$ formed on a Pb–7wt.%Sb electrode has a larger specific surface area than that formed on Pb–1wt.%Sb electrode.

4. Summary

The kinetics of the formation process of PbO$_2$ on a Pb–1wt.%Sb or a Pb–7wt.%Sb electrode have been studied with potential-step and a.c. impedance methods. The electrode has been pretreated by initial polarization at 1.3 V for 20 min and then at 0.9 V for 5 min. The electrode potential was then stepped to 1.4 or 1.3 V. With consideration of the oxidation current of the lead substrate, the current–time and the capacitance–time relationships were investigated. The formation of PbO$_2$ on a lead–antimony electrode is found to be two-dimensional instantaneous nucleation and growth process. The height of the nucleus increases with the amount of antimony, but the growth-rate constant decreases. That is, antimony enhances the formation of the PbO$_2$ nucleus, but inhibits its growth. The specific surface area of PbO$_2$ formed on Pb–7wt.%Sb electrode is larger than that for PbO$_2$ on a Pb–1wt.%Sb electrode.

References

[1] E.M.L. Valeriote and L.D. Gallop, J. Electrochem. Soc., 124 (1977) 370.
[2] J.L. Dawson, M.E. Rana and B. Munasiri, in J. Thompson (ed.), Power Sources 7, Academic Press, London, 1979, p. 1.
[3] E.J. Ritchie and J.B. Burbank, J. Electrochem. Soc., 117 (1970) 299.
[4] T. Laitinen, K. Salmi, G. Sundholm, B. Monahov and D. Pavlov, Electrochim. Acta, 36 (1991) 605.
[5] E. Hameenoja and N.A. Hampson, J. Appl. Electrochem., 14 (1984) 449.
[6] C. Wei, X.L. Chen, H.M. Li and W.F. Zhou, Acta Chim. Sinica, 47 (1989) 569.
[7] T. Laitinen and J.P. Pohl, Electrochim. Acta, 134 (1989) 3.
[8] N.A. Hampson and J.B. Lakeman, J. Electroanal. Chem., 107 (1980) 177.
[9] H.R Thirsk and J.A. Harrison, A Guide to the Study of Electrode Kinetics, Academic Press, London, 1972, p. 116.
[10] D. Pavlov, J. Power Sources, 42 (1993) 345.